Recent variability of the tropical tropopause inversion layer

Wuke Wang,[1,2] Katja Matthes,[2] Torsten Schmidt,[3] and Lisa Neef[2]

Received 18 October 2013; revised 22 November 2013; accepted 25 November 2013; published 9 December 2013.

[1] The recent variability of the tropopause temperature and the tropopause inversion layer (TIL) are investigated with Global Positioning System Radio Occultation data and simulations with the National Center for Atmospheric Research's Whole Atmosphere Community Climate Model (WACCM). Over the past decade (2001–2011) the data show an increase of 0.8 K in the tropopause temperature and a decrease of 0.4 K in the strength of the tropopause inversion layer in the tropics, meaning that the vertical temperature gradient has declined, and therefore that the stability above the tropopause has weakened. WACCM simulations with finer vertical resolution show a more realistic TIL structure and variability. Model simulations show that the increased tropopause temperature and the weaker tropopause inversion layer are related to weakened upwelling in the tropics. Such changes in the thermal structure of the upper troposphere and lower stratosphere may have important implications for climate, such as a possible rise in water vapor in the lower stratosphere. **Citation:** Wang, W., K. Matthes, T. Schmidt, and L. Neef (2013), Recent variability of the tropical tropopause inversion layer, *Geophys. Res. Lett.*, *40*, 6308–6313, doi:10.1002/2013GL058350.

1. Introduction

[2] The upper troposphere and lower stratosphere (UTLS) is a key region for troposphere-stratosphere interactions and reacts particularly sensitively to climate change [*Fueglistaler et al.*, 2009]. The tropopause inversion layer (TIL) refers to a narrow (1–2 km) band of temperature inversion above the tropopause associated with a region of enhanced static stability. It was discovered by *Birner* [2006] and confirmed by the Global Positioning System Radio Occultation (GPS-RO) data over all geographical regions [*Randel et al.*, 2007; *Grise et al.*, 2010]. The formation and maintenance of the TIL are not yet well understood, but seem to be related to dynamics [*Birner*, 2006; *Wirth and Szabo*, 2007], radiation [*Randel et al.*, 2007; *Randel and Wu*, 2010; *Schmidt et al.*, 2010a], or a combination of both [*Birner*, 2010].

[3] To improve our understanding of the TIL and its potential impact on climate, this study investigates the variability of the tropical TIL over the past decade. Such an investigation has not been possible so far, due to a lack of observational data with global coverage and sufficiently high vertical resolution over a sufficient period of time. Here we use GPS-RO data from the Challenging Minisatellite Payload (CHAMP) and Gravity Recovery and Climate Experiment (GRACE) satellites [*Schmidt et al.*, 2005; *Wickert et al.*, 2009] which are well suited for studying the TIL because they have long-term stability, are self-calibrating, and have very high vertical resolution compared to radiosondes.

[4] Coupled Chemistry Climate Models (CCMs) with fully interactive radiative, chemical and dynamical, processes are the state-of-the-art tools for investigating the variability and physical mechanisms in the stratosphere and the UTLS region. However, as reported by the Chemistry-Climate Model Validation Activity (CCMVal) of Stratospheric Processes and their Role in Climate (SPARC) [*SPARC-CCMVal*, 2010], the CCMVal-2 models may not be able to reproduce the structure of the observed TIL with quantitative accuracy due to the relatively coarse vertical resolution of standard CCMs, which is about 1 km in the UTLS. Here we run an ensemble of three simulations using a much higher vertical resolution version (about 300 m in the UTLS) of NCAR's WACCM model (WACCM-highres) to investigate the mechanism(s) for the formation of the TIL and possible reasons for its variability in the past decade.

2. Data and Model Description

2.1. GPS-RO Data

[5] The CHAMP mission has generated the first long-term GPS-RO data set (2001–2008) [*Wickert et al.*, 2001; *Schmidt et al.*, 2005, 2010b]. Besides one complete month of missing data (July 2006), CHAMP has continuously delivered between 150 and 200 temperature profiles daily and about 200 profiles per month in the tropics [*Schmidt et al.*, 2010b]. To continue the data beyond the end of the CHAMP mission in September 2008, and to fill in the missing month of the data in 2006, we also use RO data from the GRACE-A satellite, which delivers atmospheric temperature profiles with the same daily data rate. The GRACE GPS receiver and error characteristics are comparable with those of CHAMP [*Wickert et al.*, 2009]. The vertical resolution of RO measurements depends on the implemented retrieval algorithms; our current software version has a vertical resolution of about 100 m in the UTLS.

2.2. Michelson Interferometer for Passive Atmospheric Sounding Data

[6] The Michelson Interferometer for Passive Atmospheric Sounding (MIPAS) is a Fourier-Transform Infrared Spectrometer with high spectral resolution which was launched into a Sun-synchronous orbit aboard the

Additional supporting information may be found in the online version of this article.

[1]Freie Universität Berlin, Institut für Meteorologie, Berlin, Germany.
[2]GEOMAR Helmholtz-Zentrum für Ozeanforschung Kiel, Kiel, Germany.
[3]Helmholtz Zentrum Potsdam, Deutsches GeoForschungsZentrum, Potsdam, Germany.

Corresponding author: W. Wang, Freie Universität Berlin, Institut für Meteorologie, Berlin, Germany. (wwang@geomar.de)

0094-8276/13/10.1002/2013GL058350

Environmental Satellite (Envisat) on 1 March 2002 and was active until April 2012 when contact to Envisat was lost. In the UTLS region the vertical resolution of MIPAS water vapor profiles is 4 to 5 km for measurements before 2005 [*Milz et al.*, 2005] and 2.3 to 3.5 km for H_2O measurements after 2005 [*Von Clarmann et al.*, 2009]. MIPAS water vapor version V40_H2O_203 was thoroughly validated against a suite of balloon-borne and satellite data during the Measurements of Humidity in the Atmosphere and Validation Experiments 2009 (MOHAVE-2009) campaign, and no significant bias in the UTLS region was found [*Stiller et al.*, 2012]. We used data from June 2002 to April 2011, to get the highest consistence in time with the GPS-RO data.

2.3. WACCM Simulations

[7] The Whole Atmosphere Community Climate Model, version 4 (WACCM4), which is one of two available atmospheric components of the Community Earth System Model (CESM), is used here in its atmosphere-only mode. WACCM4 uses the finite-volume dynamical core with 66 standard vertical levels (about 1 km vertical resolution in the UTLS). The horizontal resolution of the WACCM4 runs presented here is $1.9° \times 2.5°$ (latitude × longitude). More details of this model are described in detail in *Garcia et al.* [2007] and *Marsh et al.* [2013]. Beside this standard version, a special version with finer vertical resolution, WACCM-highres [*Gettelman and Birner*, 2007], with 103 vertical levels and about 300 m vertical resolution in the UTLS, has been used here.

[8] An ensemble of three experiments was run over the recent decade 2001–2010 with each WACCM version (standard WACCM and WACCM-highres). Available observations of sea surface temperatures and solar fluxes were used in our simulations to produce the most realistic simulation of the climate in the past decade (2001–2010). Other forcings such as greenhouse gases (GHGs) and ozone depleting substances, were used following the Intergovernmental Panel on Climate Change RCP4.5 scenario. All forcings are the same in the standard and the finer resolution simulations. Instantaneous data were stored daily for the simulations, and the tropopause was calculated from profile to profile for both the GPS-RO data and instantaneous model data. The results presented in the following are ensemble averages for the two WACCM versions, respectively.

3. TIL Variability and Possible Reasons

3.1. TIL Structure and Variability

[9] Figure 1 shows the thermal structure around the tropopause (Figure 1a), as well as the static stability (Figure 1b) from GPS-RO and model data. Here we have used a tropopause-based average, using the tropopause calculated from profiles as a reference level, and rearranging the data to a distance-to-tropopause ordinate instead of the commonly used sea level ordinate before averaging [*Birner*, 2006]. The temperature profile averaged thus preserves the sharp tropopause, while the buoyancy frequency (N^2) jumps from a low value in the upper troposphere to a maximum around 1 km above the tropopause. To be consistent with previous TIL studies [e.g., *Birner*, 2006; *Randel et al.*, 2007], we use the lapse rate tropopause (LRT) using the standard World Meteorological Organization (WMO) lapse rate criterion [*World Meteorological Organization*, 1957], rather than the cold point tropopause (CPT) commonly used in the tropics. If we use the CPT instead of the LRT, the results are quite similar (not shown). WACCM is in general able to reproduce the quantitative structure of the TIL seen in GPS-RO data although the tropopause is not as sharp, which is especially evident in the N^2 profile. This is consistent with the recent SPARC-CCMVal report [*SPARC-CCMVal*, 2010]. The finer vertical resolution of WACCM-highres captures the TIL structure slightly better.

[10] *Randel et al.* [2007] define the strength of the TIL (STIL) as the temperature difference between the temperature at 2 km above the tropopause and the tropopause temperature (TPT) in the extratropics. In Figure 1c we use a similar definition of the STIL, but with the temperature at 1 km instead of 2 km above the tropopause, since the maximum of N^2 occurs no more than 1 km above the tropopause (Figure 1b, also *Grise et al.* [2010]) in the tropics. The maximum of N^2 is used as another indicator of STIL in Figure 1d. Figure 1c/1d indicates that the observed tropical STIL is characterized by strong year-to-year variability, and an overall decline of about 0.4 K (for temperature)/0.4×10^{-4} s^{-2} (for N^2) from 2001 through 2011. The observed decline is over 95% significant, with a correlation of 0.86 between the two time series. After extracting out the internal variability, such as the El Niño–Southern Oscillation (ENSO) and the quasi-biennial oscillation (QBO) by multiple linear regression (MLR), the STIL trend becomes somewhat weaker (not shown). However, the regression onto ENSO, the QBO, and the trend were not statistically significant, which implies that the STIL results from very complex processes and is therefore not easy to fit. WACCM generally captures a negative trend, although the decrease is not significant and the variability of the STIL in the model is larger, especially for temperature. WACCM-highres reproduces the observed features better than the standard WACCM, which shows a statistically significant downward trend.

3.2. Variability of the Tropopause Temperature

[11] The observed STIL variability of the past decade could be an indication of climate change in the tropopause region. Since the static stability is closely related to the temperature, hereafter only the temperature will be used to analyze the possible reasons for the observed STIL variability. The STIL is by definition influenced by the TPT as well as the thermal structure around the tropopause. The variability of the TPT over the same period is shown in Figure 2. The observed TPT increased significantly (about 1 K) over the past decade according to the GPS-RO data. This is consistent with the results of *Wang et al.* [2012] after the year 2000. MLR was used again to extract the internal variability due to ENSO and the QBO from the tropical TPT. The tropical TPT shows an increase of about 0.8 K over the past decade after performing the regression, which is over 95% significant (Figure S1 in the supporting information). Again, the WACCM-highres experiments capture this increase slightly better than the standard WACCM, which shows an insignificant decrease of the TPT. The significant TPT increase observed by GPS-RO is directly related to the weaker STIL, with a correlation of 0.4 (for temperature)/0.7 (for N^2) to the STIL time series. The relatively low correlation between the TPT and the STIL in temperature demonstrates again the complexity of the STIL variability, which is difficult to explain with linear regression.

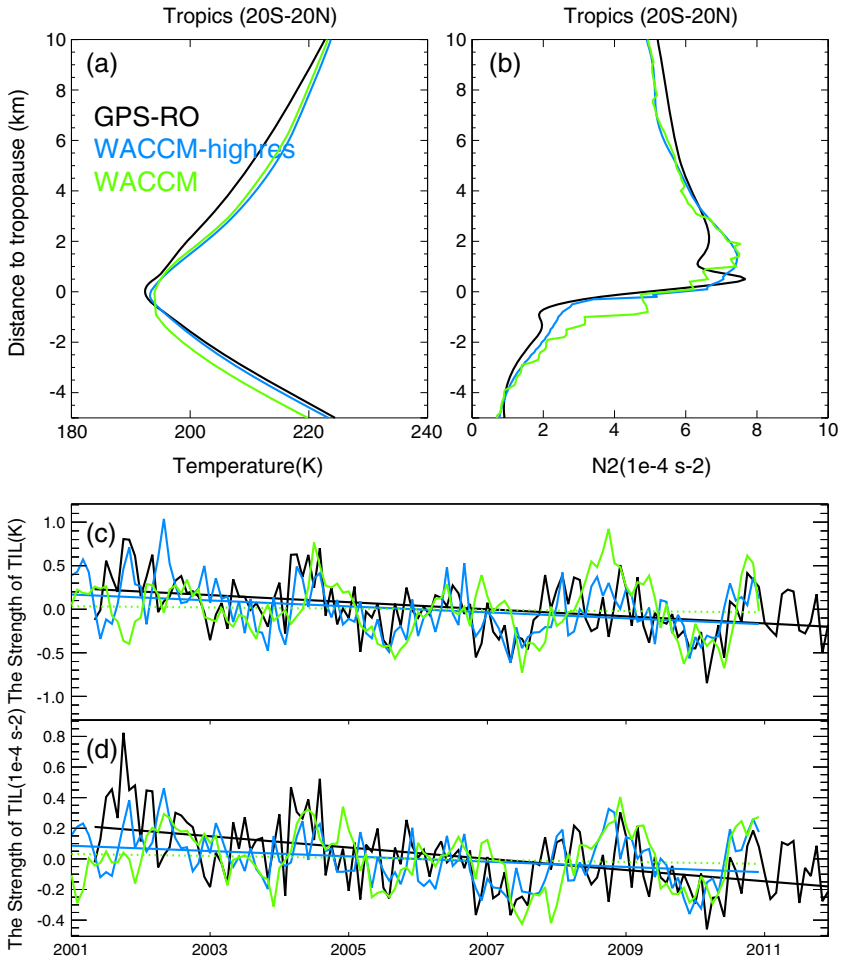

Figure 1. (a) Temperature and (b) buoyancy frequency (N^2) profiles using the tropopause as a reference level (see text for details), averaged for GPS-RO profiles and instantaneous output data from WACCM for 2001–2010. Deseasonalized monthly mean anomalies of tropical strength of TIL (STIL), (c) temperature, (d) N^2. The black, blue, and green lines represent the data from GPS-RO, WACCM-highres, and WACCM, respectively. The solid/dashed line styles for the trendlines represent trends found to be more than/less than 95% statistically significant.

[12] This warmer tropopause could be a climate change signal and is very important, since the TPT is the key determinant of how tropospheric trace gases such as water vapor are transported into the stratosphere. If the tropopause is changing, this immediately influences stratospheric water vapor content, which is important for global warming [*Solomon et al.*, 2010]. The temperature 1 km above the tropopause shows a similar but weaker increase over the

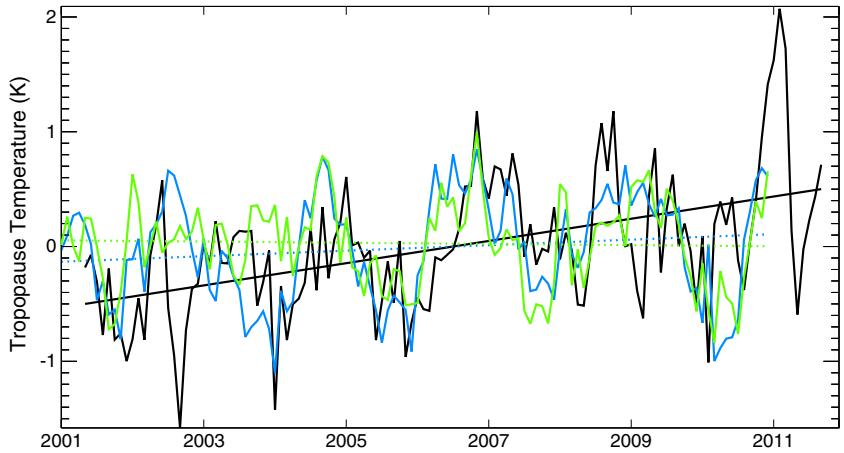

Figure 2. Deseasonalized monthly mean anomalies of the TPT in the tropics (20°S–20°N). Line colors and styles as in Figure 1.

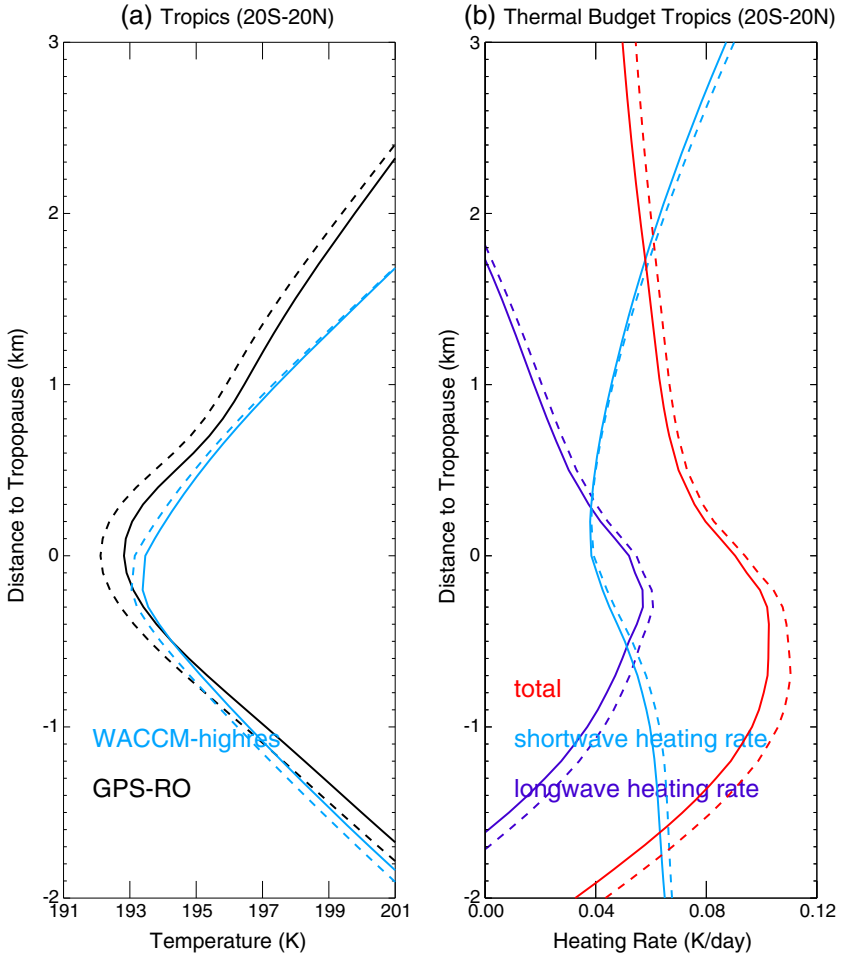

Figure 3. (a) Temperature profiles around the tropopause averaged over the first 5 years (2001–2005, dashed line) and the last 5 years (2006–2010, thick line) of the last decade from the GPS-RO data and the WACCM-highres simulations. (b) Same as Figure 3a but for different radiative heating rates from the WACCM-highres simulations.

same period (not shown). The strong increase of the TPT, and the weaker increase of the temperature 1 km above the tropopause, are the primary reasons for the decrease of the STIL.

3.3. Possible Reasons for Observed STIL Decline and TPT Increase

[13] Radiative heating rates, as well as temperature profiles around the tropopause, are shown in order to investigate the contribution of radiative effects on the temperature evolution. Figure 3a shows tropopause-based temperature profiles averaged from the first 5 years (2001–2005, dashed line) and the last 5 years (2006–2010, thick line). Clear temperature differences (over 95% confidence) between the first and last 5 years of the past decade exist in the troposphere, across the tropopause, and up to about 3 km above the tropopause in both GPS-RO and WACCM-highres data. This temperature increase over the past decade around the tropopause has been discussed by *Schmidt et al.* [2010b], though the explanation for it is still unclear.

[14] Figure 3b shows a decline (95% confidence) in the long-wave heating rates around the tropopause for the WACCM-highres simulations, and no significant changes in the short-wave heating, which results in net cooling. Please note that the radiative forcings used in our WACCM simulations, such as GHGs and aerosols are not entirely based on observations. However, the WACCM-highres simulation indicates that the warming around the tropopause is caused to a lesser extent by radiative effects, and more by a warming effect from dynamical transport or convection. Please also find the dynamical heating rates and the whole thermal budget from the WACCM-highres simulations in Figure S2. A dynamical warming can be seen clearly, and this leads to a net warming from 15 to 20 km.

[15] To better understand these dynamical changes, the vertical component of the Brewer-Dobson circulation (w*) is calculated approximately, using the Transformed Eulerian Mean method [*Edmon et al.*, 1980]. The deseasonalized monthly mean anomalies of the tropical w* from 2001 to 2010, averaged between 100–70 hPa and 20°S–20°N, are shown in Figure 4a. The WACCM-highres simulations (blue) show a slight but statistically significant decrease of w* in the tropics. A weaker w* means less upwelling and hence less cooling above the tropopause, which may result in a relative warming effect. There is also a strong correlation (0.8 with the TPT lagged by 1 month) between w* and the TPT time series. Therefore, it is possible that the increase in the TPT as well as the warming around the tropopause (Figure 3a, also seen in *Schmidt et al.* [2010b]) are an effect of a weaker Brewer-Dobson circulation. w*

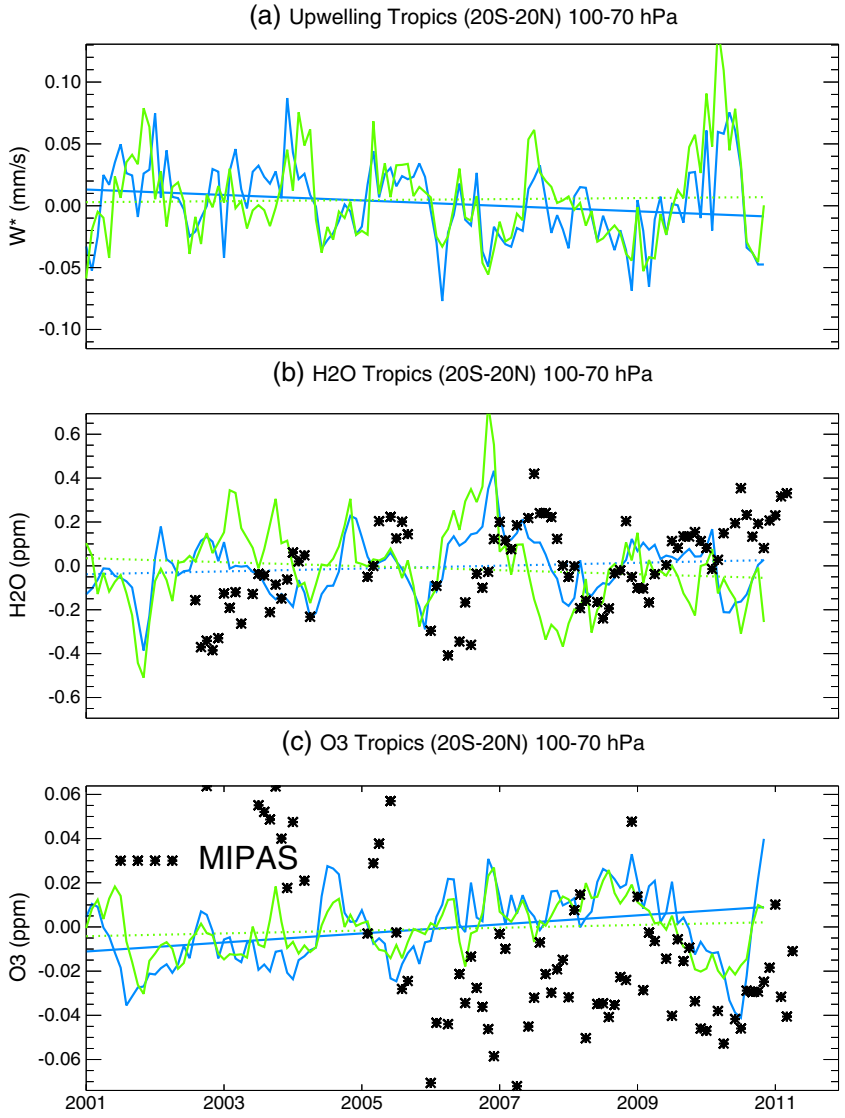

Figure 4. Deseasonalized monthly mean anomalies of (a) tropical upwelling w* (calculated from monthly mean output of the ensemble of the WACCM simulations), and (b) tropical water vapor and (c) ozone, from both MIPAS and the WACCM simulations, averaged between 100–70 hPa. Line colors and styles as in Figure 1.

from the standard WACCM simulations (green) shows a very slight, insignificant increase, which indicates the importance of high vertical resolution for simulating the dynamical transport through the UTLS.

[16] Water vapor is one of the most important gases for the formation of the TIL because of its strong radiative effects [*Randel and Wu*, 2010]. On the other hand, the magnitude of stratospheric water vapor is strongly dependent on the TPT [*Rosenlof and Reid*, 2008], which determines the transport of water vapor from the troposphere to the stratosphere. Figure 4b shows the evolution of tropical water vapor above the tropical tropopause (100–70 hPa 20°S–20°N) in the past decade, from MIPAS and the two ensemble mean WACCM simulations. Overall, the tropical water vapor in the lower stratosphere slightly increased over the past decade according to the MIPAS data and the WACCM-highres simulations, but slightly decreased in the standard WACCM run. This increase of tropical water vapor in the lower stratosphere was also shown by previous studies [*Solomon et al.*, 2010; *Hurst et al.*, 2011]. Even though water vapor shows relatively large differences between the different data sets mentioned above, WACCM-highres reproduces an absolute value closer to the MIPAS data than the standard WACCM (not shown). This enhanced water vapor most likely results from the increased TPT, but whether the weaker STIL that also contributes is still unclear. Furthermore, the potential effects of enhanced water vapor on the thermal structure around the TIL are also not yet understood. Not only the magnitude, but also the gradient of water vapor above the tropopause, influences the TIL structure.

[17] Ozone concentration is also argued to be important for the TIL formation [*Randel et al.*, 2007]. Figure 4c shows a significant increase of ozone in the lower stratosphere from the WACCM-highres simulations, which is consistent with the recent work by *Gebhardt et al.* [2013]. The MIPAS ozone data show different tendencies between the first (2002–2005) and the following (2006–2010) time periods, making it difficult to fit a linear trend. The increased

ozone in the WACCM-highres simulation might be caused by the weakened upwelling and may also be important for the UTLS thermal structure.

4. Summary and Outlook

[18] A decrease in tropical STIL of 0.4 K and an increase in tropical TPT of 1 K (or 0.8 K after extracting the contributions from ENSO and QBO by the MLR) over the last decade were found in the GPS-RO data from CHAMP and GRACE. A WACCM simulation with high vertical resolution reproduces the TIL sharpness and variability better than the standard WACCM with coarser vertical resolution in the UTLS. The decrease of the STIL and the increase of the TPT are directly related to each other and are a combination of both dynamical and radiative processes. Weaker upwelling might lead to a warmer tropopause and less cooling or even warming of the lower stratosphere. However, the increase of tropical TPT and the decline in upwelling can only be shown in the WACCM-highres but not in the standard WACCM simulation. This will need to be checked again in more simulations and indicates more uncertainty in our explanation of the recent UTLS variability. The warmer tropopause leads to enhanced water vapor and may have subsequent radiative effects in the lower stratosphere. This trend analysis is still relatively uncertain, since we only have about 10 years of observations. The explanation for the recent UTLS variability is still not clear. Further work is necessary to diagnose the relative contribution from different factors.

[19] Similar decreases of the STIL can also be found in other latitudes (not shown) and will be discussed in a future study. It will be also important to quantitatively analyze and understand the mechanisms for the TIL formation, and its potential importance for climate change in more detail.

[20] **Acknowledgments.** W. Wang is supported by a fellowship of the China Scholarship Council (CSC) at FU Berlin. This work was also performed within the Helmholtz-University Young Investigators Group NATHAN, funded by the Helmholtz-Association through the presidents Initiative and Networking Fund, and the GEOMAR - Helmholtz-Zentrum für Ozeanforschung in Kiel. We thank Gabriele Stiller and the MIPAS-Envisat team at the Karlsruhe Institute of Technology for the provision of and insights into the MIPAS data. We thank Andrew Gettelman and Dan Marsh from NCAR for their help in setting up the WACCM high resolution model runs, as well as Markus Kunze from FU Berlin for providing us the MLR code. The model calculations have been performed at the Deutsche Klimarechenzentrum (DKRZ) in Hamburg, Germany.

[21] The Editor thanks two anonymous reviewers for their assistance in evaluating this paper.

References

Birner, T. (2006), Fine-scale structure of the extratropical tropopause region, *J. Geophys. Res.*, *111*, D04104, doi:10.1029/2005JD006301.

Birner, T. (2010), Residual circulation and tropopause structure, *J. Atmos. Sci.*, *67*, 2582–2600, doi:10.1175/2010JAS3287.1.

Edmon, H., B. Hoskins, and M. McIntyre (1980), Eliassen-palm cross sections for the troposphere, *J. Atmos. Sci.*, *37*(12), 2600–2616, doi:10.1175/1520-0469(1980)037<2600:EPCSFT>2.0.CO;2.

Fueglistaler, S., A. Dessler, T. Dunkerton, I. Folkins, Q. Fu, and P. W. Mote (2009), Tropical tropopause layer, *Rev. Geophys.*, *47*, 1004, doi:10.1029/2008RG000267.

Garcia, R., D. Marsh, D. Kinnison, B. Boville, and F. Sassi (2007), Simulation of secular trends in the middle atmosphere, 1950–2003, *J. Geophys. Res.*, *112*, D09301, doi:10.1029/2006JD007485.

Gebhardt, C., A. Rozanov, R. Hommel, M. Weber, H. Bovensmann, J. P. Burrows, D. Degenstein, L. Froidevaux, and A. M. Thompson (2013), Stratospheric ozone trends and variability as seen by SCIAMACHY during the last decade, *Atmos. Chem. Phys. Discuss.*, *13*, 11,269–11,313, doi:10.5194/acpd-13-11269-2013.

Gettelman, A., and T. Birner (2007), Insights into tropical tropopause layer processes using global models, *J. Geophys. Res.*, *112*, D23104, doi:10.1029/2007JD008945.

Grise, K. M., D. W. Thompson, and T. Birner (2010), A global survey of static stability in the stratosphere and upper troposphere, *J. Clim.*, *23*, 2275–2292, doi:10.1175/2009JCLI3369.1.

Hurst, D. F., S. J. Oltmans, H. Vömel, K. H. Rosenlof, S. M. Davis, E. A. Ray, E. G. Hall, and A. F. Jordan (2011), Stratospheric water vapor trends over Boulder, Colorado: Analysis of the 30 year Boulder record, *J. Geophys. Res.*, *116*, D02306, doi:10.1029/2010JD015065.

Marsh, D. R., M. J. Mills, D. E. Kinnison, J.-F. Lamarque, N. Calvo, and L. M. Polvani (2013), Climate change from 1850 to 2005 simulated in CESM1 (WACCM), *J. Clim.*, *26*, 7372–7391, doi:10.1175/JCLI-D-12-00558.1.

Milz, M., et al. (2005), Water vapor distributions measured with the Michelson interferometer for passive atmospheric sounding on board Envisat (MIPAS/Envisat), *110(D9)*, *24*, D24307, doi:10.1029/2005JD005973.

Randel, W. J., and F. Wu (2010), The polar summer tropopause inversion layer, *J. Atmos. Sci.*, *67*, 2572–2581, doi:10.1175/2010JAS3430.1.

Randel, W. J., F. Wu, and P. Forster (2007), The extratropical tropopause inversion layer: Global observations with GPS data, and a radiative forcing mechanism, *J. Atmos. Sci.*, *64*, 4489–4496.

Rosenlof, K. H., and G. C. Reid (2008), Trends in the temperature and water vapor content of the tropical lower stratosphere: Sea surface connection, *J. Geophys. Res.*, *113*, D06107, doi:10.1029/2007JD009109.

Schmidt, T., J. Wickert, G. Beyerle, R. König, R. Galas, and C. Reigber (2005), The CHAMP atmospheric processing system for radio occultation measurements, in *Earth Observation With CHAMP: Results From Three Years in Orbit*, edited by C. Reigber et al., pp. 597–602, Springer, Berlin.

Schmidt, T., J.-P. Cammas, H. Smit, S. Heise, J. Wickert, and A. Haser (2010a), Observational characteristics of the tropopause inversion layer derived from CHAMP/GRACE radio occultations and MOZAIC aircraft data, *J. Geophys. Res.*, *115*, D24304, doi:10.1029/2010JD014284.

Schmidt, T., J. Wickert, and A. Haser (2010b), Variability of the upper troposphere and lower stratosphere observed with GPS radio occultation bending angles and temperatures, *Adv. Space. Res.*, *46*, 150–161, doi:10.1016/j.asr.2010.01.021.

Solomon, S., K. H. Rosenlof, R. W. Portmann, J. S. Daniel, S. M. Davis, T. J. Sanford, and G.-K. Plattner (2010), Contributions of stratospheric water vapor to decadal changes in the rate of global warming, *Science*, *327*, 1219–1223, doi:10.1126/science.1182488.

Stratospheric Processes and their Role in Climate–Chemistry-Climate Model Validation Activity (SPARC-CCMVal) (2010), SPARC report on the evaluation of chemistry-climate models, in *SPARC Report No. 5, WCRP-132,* WMO/TD-No. 1526, edited by V. Eyring, T. G. Shepherd, and D. W. Waugh, available at: http://www.sparc-climate.org/publications/sparc-reports/sparc-report-no5/.

Stiller, G., et al. (2012), Validation of MIPAS IMK/IAA temperature, water vapor, and ozone profiles with MOHAVE-2009 campaign measurements, *Atmos. Meas. Tech.*, *5*, 289–320, doi:10.5194/amt-5-289-2012.

Von Clarmann, T., et al. (2009), Retrieval of temperature, H_2O, O_3, HNO_3, CH_4, N_2O, $ClONO_2$ and ClO from MIPAS reduced resolution nominal mode limb emission measurements, *Atmos. Meas. Tech.*, *2*, 159–175, doi:10.5194/amt-2-159-2009.

Wang, J. S., D. J. Seidel, and M. Free (2012), How well do we know recent climate trends at the tropical tropopause?, *J. Geophys. Res.*, *117*, D09118, doi:10.1029/2012JD017444.

Wickert, J., et al. (2001), Atmosphere sounding by GPS radio occultation: First results from CHAMP, *Geophys. Res. Lett.*, *28*(17), 3263–3266, doi:10.1029/2001GL013117.

Wickert, J., et al. (2009), GPS radio occultation: Results from CHAMP, GRACE and FORMOSAT-3/COSMIC, *Terr. Atmos. Oceanic Sci.*, *20*(1), 35–50, doi:10.3319/TAO.2007.12.26.01(F3C).

Wirth, V., and T. Szabo (2007), Sharpness of the extratropical tropopause in baroclinic life cycle experiments, *Geophys. Res. Lett.*, *34*, L02809, doi:10.1029/2006GL028369.

World Meteorological Organization (1957), Meteorology–A three-dimensional science, *WMO Bull*, *6*, 134–138.